Talanta Open 8 (2023) 100250

Contents lists available at ScienceDirect

Talanta Open

journal homepage: www.sciencedirect.com/journal/talanta-open

Additive manufacturing of carbon black immunosensors based on covalent immobilization for portable electrochemical detection of SARS-CoV-2 spike S1 protein

Luiz Ricardo Guterres Silva [a], Jéssica Santos Stefano [a,*], Robert D. Crapnell [b], Craig E. Banks [b], Bruno Campos Janegitz [a,*]

[a] Laboratory of Sensors, Nanomedicine, and Nanostructured Materials (LSNano), Federal University of São Carlos, Araras, São Paulo 13600-970, Brazil
[b] Faculty of Science and Engineering, Manchester Metropolitan University, Chester Street, Manchester M1 5GD, United Kingdom

ARTICLE INFO

Keywords:
Additive manufacturing
3D printed electrochemical (bio)sensor
Immunosensor
SARS-CoV-2
Spike S1 protein

ABSTRACT

The global pandemic of the COVID-19 disease has emphasized the need to develop clinical tests which are simple, fast and inexpensive. In this aspect, electrochemical biosensors are alternatives capable to attend such requirements and providing reliable results, highly required in clinical analysis. Associating the quality of electrochemical biosensors with additive manufacturing technology (3D printing) ensures the production of sensors on a large scale, at a reduced cost, and in an automated way. In this regard, the present work proposes the development of an additive-manufactured electrochemical immunosensor, based on the covalent immobilization of antibodies on electrodes obtained from lab-made conductive filaments, composed of carbon black and polylactic acid, for the detection of the spike S1 protein of the SARS-CoV-2 virus. Due to the readily available carboxylic groups on the surface of the additive-manufactured sensor, it was possible to produce an immunosensor without the need for modification steps with metallic particles. Therefore, the proposed immunosensor showed satisfactory results, with a linear range varying from 0.01 to 4.5 nmol L^{-1} and a detection limit of 2.7 pmol L^{-1}, with a sensitivity of 7.606 μA $nmol^{-1}$ L. The 3D-printed immunosensor was fully designed for *in loco* application and all results were obtained from portable equipment, making it a highly viable alternative to be applied as a point-of-care device.

Introduction

The end of 2019 was marked by the emergence of a new respiratory virus denominated SARS-CoV-2. This virus is the cause of the disease known as COVID-19, which led to the beginning of a new global pandemic in 2020 [1]. Due to the emergence of this virus, hundreds of millions of cases of infected people have already been registered, causing millions of deaths. Facing this serious public health problem, efforts have been made to mitigate the effects of this disease since the beginning of the pandemic, and one of the main allies in the fight against COVID-19 is the development of clinical tests capable of detecting the SARS-CoV-2 virus in biological samples [2–5]. Mass clinical tests allow the competent authorities to take the necessary contingency measures and actions to reduce the spread of the virus [2,4,5]. Nevertheless, current clinical trials, even having excellent qualities and considering their important role during the pandemic, still have some disadvantages. In this context, it can be mentioned the cost, long analysis time, sophisticated equipment and the need for specialized labor [2,6]. Thus, several countries do not have the resources and infrastructure to efficiently use these tests and control a virus spreading. Thus, the development of new clinical tests has gained prominence and shown great potential, with several efforts and research to obtain high-quality and reliable tests [5,7–9].

New tests and analytical platforms need to meet some requirements to be used in clinical tests, such as simplicity, fast analysis, low cost, the possibility of being used at the bedside and not needing a specialized operator [10–12]. By fulfilling these requirements, these new devices contribute to combating the pandemic efficiently, since they become viable alternative options. Also, these tools can easily applied *in loco*, which contribute to a fairer society that is often deprived of such public health actions [11,13]. In this way, electrochemical immunosensors are a highly viable alternative as they can be employed to perform analysis

* Corresponding authors.
E-mail addresses: jessica.s.stefano@gmail.com (J.S. Stefano), brunocj@ufscar.br (B.C. Janegitz).

https://doi.org/10.1016/j.talo.2023.100250
Received 6 April 2023; Received in revised form 19 July 2023; Accepted 5 August 2023
Available online 6 August 2023

quickly and simply, requiring a low volume of samples and reagents, and showing the possibility of being portable and miniaturized, allowing point-of-care analysis [6,14,15]. In this context, developing new electrochemical immunosensors for virus detection, such as SARS-CoV-2, has great potential due to its advantageous characteristics, mainly about not requiring a specialized operator and application in loco [6]. Furthermore, it is possible to employ new technologies for the production of such electrochemical sensors. The additive manufacturing technology is a powerful ally for the production of electrochemical (bio) sensors, since it allows fast, low-cost, automated, *in loco* manufacturing, with varied sizes and designs of (bio)sensors [16–18].

Additive manufacturing has shown great potential for the construction of electrochemical devices and sensors for diverse analysis applications such as biomarkers, metals, illicit drugs, explosives, neurotransmitters, pesticides, H_2O_2, glucose, and viruses [18–22]. Despite showing wide applicability, additive manufacturing is still in its infancy for use in analytical chemistry, more specifically in the manufacture of electrochemical sensors and the production of electrochemical biosensors [16,23,24]. In the literature, there are only a few reports on the production of additive manufacturing electrochemical biosensors, mainly compared to conventional electrodes such as glassy carbon, carbon paste, or screen-printed electrodes.

One of the first additive manufacturing electrochemical immunosensor for viruses reported in the literature was presented by Martins et al., 2020 for the detection of Hantavirus disease [25]. The work presents an electrochemical immunosensor based on the direct immobilization of Hantavirus Araucaria antibodies onto a commercial 3D conductive filament of carbon black and polylactic acid (PLA). Regarding the detection of the SARS-CoV-2 virus, some electrochemical biosensors have been reported in the literature, including immunosensors. Munoz and Pumera, 2021 [26], presented the first 3D-printed immunosensor for the detection of the SARS-CoV-2 virus. In their work, a 3D-printed sensor based on commercial filaments containing graphene and PLA was developed. The obtained electrodes were modified with gold nanoparticles and biological material, in this case, a specific antibody for detecting the biomarker/antigen. Another interesting work was presented by Stefano et al., 2022 [27], which produced a new conductive filament for the manufacture of 3D-printed electrochemical sensors based on graphite and PLA. As a proof of concept, the new 3D-printed sensors were applied for the immunodetection of SARS-CoV-2 spike protein in synthetic saliva.

Although additive manufacturing presents excellent results in the production of electrochemical (bio)sensors, there is still much to be studied, researched, and explored. Works such as those developed Kalinke et al., 2023 [28] and Morawski et al., 2023 [29] which successfully managed to show the versatility of this fast and economical prototyping technology are just the tip of the iceberg. Thus, looking for new materials for the production of sensors, different strategies, prototyping, and analytical platforms is highly advantageous and presents great potential both for the academic area and for clinical analysis. In this context, bespoke filaments based on carbon black is an interesting and high-potential proposal, which is still little explored. Therefore, developing new 3D printed (bio)sensors based on bespoke filaments becomes a hot topic, especially for high-relevance analytes such as the SARS-CoV-2 virus.

Therefore, in the present work, a bespoke filament based on carbon black and PLA was used to develop a fully 3D printed electrochemical immunosensor for the detection of the SARS-CoV-2 virus. The main steps of immunosensor production were fully optimized by design of experiments. In addition, a new 3D printed electrochemical cell design was also developed for the analysis of small amounts of samples (100 μL). The cell was designed to be similar the configuration of disposable commercial electrodes (screen-printed electrodes). Also, the present work demonstrates the feasibility of developing a biosensor from conductive filaments entirely produced in the laboratory by a simple and accessible production route.

Experimental

Reagents and solutions

All chemicals used in this work were of analytical grade, and the solutions were prepared using ultra-pure water with a resistivity higher than 18.0 MΩ cm from a Milli Q water purification system from Millipore (MA, USA). Potassium chloride (99% w/w), ferrocenemethanol (FcMeOH) (97% w/w), N-(3-dimethylaminopropyl)-N'- ethylcarbodiimide hydroxchloride (EDC) (98% w/w) and N- hydroxysuccinimide (NHS) (98% w/w), purchased from Sigma- Aldrich® (St. Louis, USA), were employed in the construction and electrochemical evaluation of the immunosensor. For the diagnosis of COVID-19, a recombinant SARS-CoV-2 spike (S1) (antigen) and a SARS-CoV-2 spike antibody (S1 Ab) were used, which were acquired both from Sino Biological (Wayne, USA).

Synthetic saliva was prepared following the literature [30], with adaptations, which was composed of a mixture of 0.7 g L^{-1} sodium chloride (99% w/w), 1.2 g L^{-1} potassium chloride (99% w/w), 0.26 g L^{-1} sodium phosphate dibasic (99% w/w), 0.33 g L^{-1} potassium thiocyanate, and 1.3 g L^{-1} urea (99% w/w). For this purpose, all reagents were purchased from Vetec® (São Paulo, Brazil) and solubilized in water. Human serum was obtained from Sigma- Aldrich® (St. Louis, USA). For SARS-CoV-2 analysis, human serum was diluted 1:100 in PBS 1 × . Then, the samples were enriched with three different concentrations of antigen (0.05, 0.1, and 1.0 nmol L^{-1}).

Instrumental and apparatus

All electrochemical tests were carried out using a μSTAT i-400 portable potentiostat (Metrohm DropSens®, Spain) controlled by a laptop, with Windows 10® operating system (Intel core I5 processor and 8.0 GB RAM), through the Dropview 8400® software. A Sethi3D S3 3D printer (Campinas, Brazil) was used for printing the structures and electrodes, controlled by the software Simplify 3D™. A Filmaq3D® extruder (Curitiba, Brazil) was used for the extrusion of the obtained composites. Scanning electron microscopy (SEM) analyzes were performed using a Thermo Fisher Scientific model Prisma E for characterization. Voltammetric characterizations were performed using cyclic voltammetry.

Composite filament and CB-PLA electrodes

The electrodes employed in this work were additively manufactured from a lab-made composite filament composed of PLA and carbon black (CB) (28.5% wt.), which was called CB-PLA, obtained following previous work from our research group [19,27]. For this, pellets of PLA were dissolved in a mixture of solvents (acetone/chloroform, 4:1 v/v), with subsequent incorporation of CB under a reflux system (70 °C under stirring) for 3 h. The composite was obtained by recrystallization in ethanol and posteriorly dried in the oven at 50 °C for 12 h. The extrusion of the composite was performed at 180 °C to provide the conductive filaments based on CB. The PLA used to manufacture the composite filaments was obtained as pellets *in natura*, from 3DLAB (Minas Gerais, Brazil) and Carbon black (VULCAN® XC-72R) from Cabot (São Paulo, Brazil).

After extrusion, the filaments were coupled to the 3D printer to obtain the working, counter, and pseudo-reference electrodes. For printing the electrodes, an extrusion nozzle of 0.4 mm in width was used, with printing temperature and table of 240.0 and 75 °C, respectively. The layer height was 0.1 mm, with a printing speed of 500.0 mm/min. The working electrode was printed with a working area of 4.0 mm and the connection length of all electrodes was 2.0 cm. The connection length of the electrodes was defined based on the work described by Crapnell et al., 2022 [31], in which the shorter the connection length of the sensors, the lower the charge transfer resistance. Thus, considering

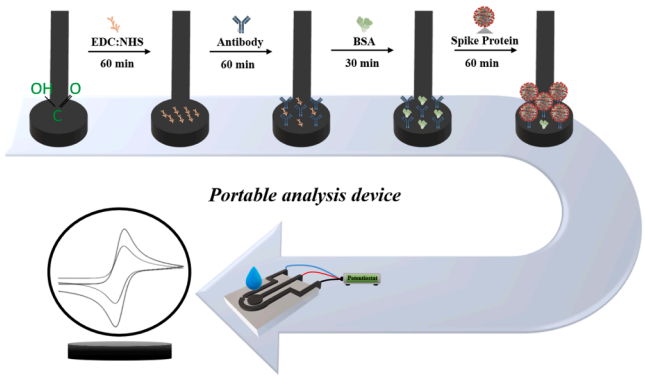

Fig. 1. Scheme of all steps involved in the construction of the electrochemical immunosensor and conception of the real design of the electrochemical sensor. The steps taken were immobilization of EDC:NHS on the surface for 60 min; antibody anchoring for 60 min; blocking of non-binding sites for 30 min and finally, detection of Spike S1 protein in the proposed samples after 60 min.

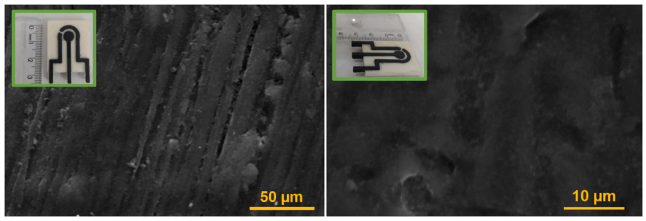

Fig. 2. SEM images for CB-PLA sensors, with amplification factors of 1000 × (50 µm scale) and 4000 × (10 µm scale). Inset: real conception of the manufactured sensors.

the manufactured electrochemical platform, the smallest possible connection length to be used was 1.5 cm. A simple mold was produced using white acrylonitrile butadiene styrene (ABS) filament for coupling the electrodes and closing the electrochemical system by using a drop (100 µL) of supporting electrolyte capable of covering the three electrodes. Previous to the biosensor fabrication, each electrode was simply mechanically polished using humid sandpaper (grit 1200).

Biosensor preparation

To prepare the immunosensor, initially, the antibodies were covalently bonded to the working electrode surface, using 10 µL of a solution containing 10.0 mmol L^{-1} EDC and 20.0 mmol L^{-1} NHS in PBS 1× (pH = 7.4), dropped directly at the electrode surface and rested for 60 min, followed by 60 min immobilization of 1.8 µg mL^{-1} antibody solution (10 µL) in PBS 1 × (pH = 7.4). The step of the antibody immobilization on the sensor surface was optimized using multivariate optimization. For this, the Central Composite Design (CCD) planning was applied for the variable's antibody concentration and incubation time. Variables were studied in the range of 0.6 to 2.4 µg mL^{-1} and 36 to 144 min, for antibody concentration and incubation time, respectively. The subsequent drop-casting of 10 µL BSA solution (1% w/v) in PBS 1x (pH = 7.4) was performed and incubated for 30 min to block any interaction sites available in the CB- PLA. The electrode was rinsed after each step with PBS 1× and dried in air. After that, the immunosensor was ready for the detection of the virus spike protein. The detection was performed upon 60 min incubation of different concentrations of antigen diluted in PBS 1x (pH = 7.4). All experiments were performed at room temperature. Fig. 1 presents a representative scheme of the steps involved in the fabrication of the 3D-printed electrochemical immunosensor, and an illustration of the electrochemical system used for the analysis.

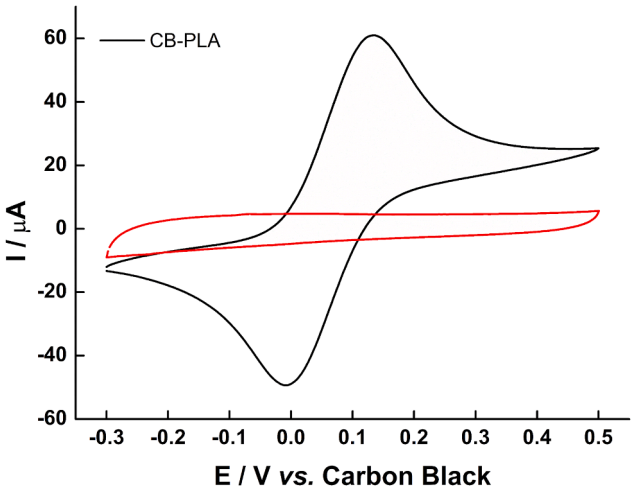

Fig. 3. (a) Cyclic voltammetric recorded in the presence of 1.0 mmol L^{-1} FcMeOH in 0.1 mol L^{-1} KCl. Scan rate: 50 mV s^{-1}.

Results and discussion

The electrochemical sensor was designed for the use of small volumes of solution or sample, requiring only 100 µL. Furthermore, its connectors were designed aiming for a satisfactory space in between, to facilitate the connection with potentiostats alligators. After printing the electrochemical sensors, the morphological characterization of the sensors was carried out using SEM. Fig. 2 presents images of the surface with different magnifications (1000 and 4000 ×).

In Fig. 2, it is possible to observe that at 1000 × magnification (50 µm scale) the sensor presents a flat and homogeneous surface, demonstrating the good efficiency of the printing process, with the absence of holes. At 4000 × magnification (10 µm scale) it is possible to observe a less homogeneous appearance and some possible porosities referring to the presence of CB in the material. In addition, no sophisticated pretreatment steps were used (a simple mechanical polishing) to eliminate PLA from the surface the polymer is essential for the construction of the immunosensor. Also, it is possible to observe "smooth" and continuous layers in the amplified image. The certain smoothness observed in some points, covering the surface, can be attributed to the PLA present in the material. Thus, it is possible to infer that even after mechanical polishing, both PLA and CB are present on the surface in "balanced" proportions. In this regard, we prepared an immunosensor based on covalent bonding at the PLA (rich in carboxylic groups), allowing the detection by the monitoring of a redox probe after partial blockage of the conductive CB from the surface.

For the voltammetric analysis, CV was initially performed in the presence of 1.0 mmol L^{-1} FcMeOH in 0.1 mol L^{-1} KCl. Fig. 3 shows the voltammogram. The voltammetric response showed an oxidation and a reduction peak at potentials of +0.13 and −0.01 V, respectively, corresponding to a ΔEp of 0.131 V. Also, the cathodic peak is slightly lower in intensity compared to the anodic peak, showing a ratio between the cathodic and anodic peak current of 1.07. Thus, the sensor response in the presence of the redox probe presented a quasi-reversible behavior, commonly reported in the literature for FcMeOH using 3D printed electrodes [19,27,32]. Thus, it is possible to observe that even without the application of any surface treatment, and from just a simple mechanical polishing process is possible to anchor the biological materials, once the proposed sensor presented an electrochemical response in the presence of the proposed redox.

The estimative of the apparent electroactive area was performed using the Randles-Ševčíck equation for quasi-reversible systems [33]. Fig. S1 presents the voltammograms obtained and the relationship between the peak current (anodic and cathodic) and the square root of the

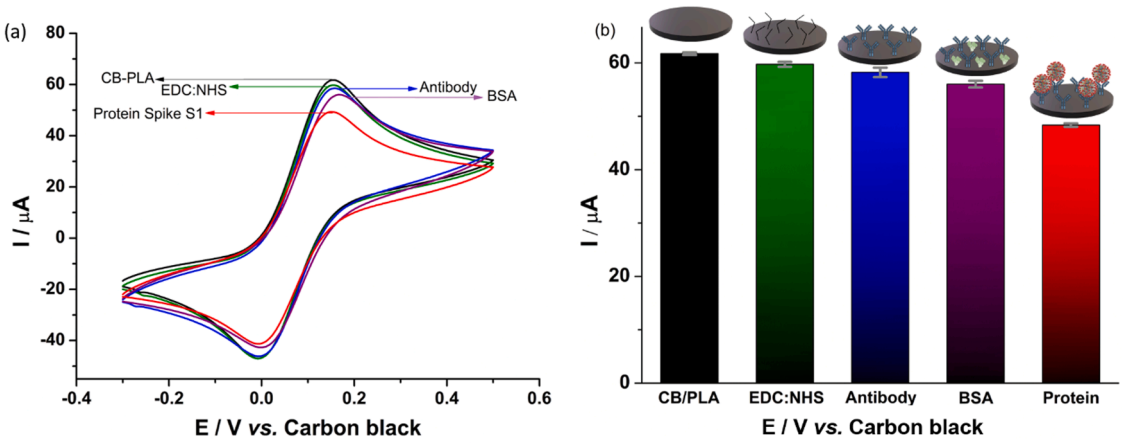

Fig. 4. (a) Cyclic voltammetric recordings in the presence of 1.0 mmol L^{-1} FcMeOH in 0.1 mol L^{-1} KCl after each immobilization step (black line) CB-PLA, (green line) EDC:NHS, (blue line) antibody, (purple line) BSA and (red line) detection of 1.0 nmol L^{-1} antigen. Scan rate: 50 mV s^{-1}, and (b) Respective peak current values.

scan rate used in the study (10 to 100 mV s^{-1}). The diffusion coefficient of the redox probe used in the calculation was 7.6 × 10^{-6} cm^2 s^{-1} [34]. The calculated electroactive surface area showed a value of 25.1 mm^2. The real geometric area of the 3D printed sensor is approximately 12.5 mm^2, therefore, the electroactive area is 2.0-fold higher than the real geometric area of the electrode. This considerable difference between the geometrical and the apparent electroactive area is possibly due to a roughness of the sensor surface with active sites containing CB particles present in the sensor matrix. However, because the sensor has PLA in a considerable proportion on the surface of the sensor, it is not possible to accurately estimate the roughness of the sensor. Thus, the bespoke filament based on CB and PLA showed potential to be a platform for manufacturing an immunosensor based on covalent bonding. In fact, the conductive surface provides satisfactory voltammetric responses in the presence of the redox probe, while the PLA on the surface is capable of performing the necessary covalent bonding to further attachment of the antibodies.

For the monitoring of each step involved in the production of the immunosensor and the analysis of the spike S1 protein was carried out. For this, the cyclic voltammetric technique was used employing a 1.0 mmol L^{-1} FcMeOH solution prepared in 0.1 mol L^{-1} KCl, at a scan rate of 50 mV s^{-1}. The voltammograms were recorded after each stage of biosensor preparation, namely binding of EDC:NHS, immobilization of the specific antibody, blocking of non-binding sites, and finally the detection of the spike protein of the virus. The direct binding of EDC:NHS to the sensor surface was possible due to the presence of carboxylic groups on the sensor surface, previously reported in the literature [19,27]. The possibility of direct covalent linking EDC:NHS on the electrode is of paramount importance as it avoids additional steps involving modification with other materials, saving time in the preparation of the biosensor, and providing a simpler and lower-cost biosensing platform [35]. Fig. 4 presents the voltammetric responses obtained as well as the peak currents of each step performed.

From Fig. 4, it is possible to observe the typical oxidation and reduction peaks of the redox probe. When the layers were added to the CB-PLA sensor, the peak current decreased. This current decrease is caused by the deposition of biological material on the surface of the CB-PLA, which resulted in a partial "blocking" of active sites of the electrochemical sensor. In addition, in the last step after the incubation of 1.0 nmol L^{-1} Spike S1 protein from the SARS-CoV-2 virus, a more pronounced decrease of the peak current occurred, demonstrating the efficiency of the sensor in detecting the antigen of interest, from the proposed bio-complexation reaction (antigen-antibody). Thus, from the peak current difference in the absence (CB-PLA/EDC:NHS/Ab/BSA) and the presence of antigen (CB-PLA/EDC:NHS/Ab/BSA/Ag), it is likely that it is possible to correlate with the antigen concentration.

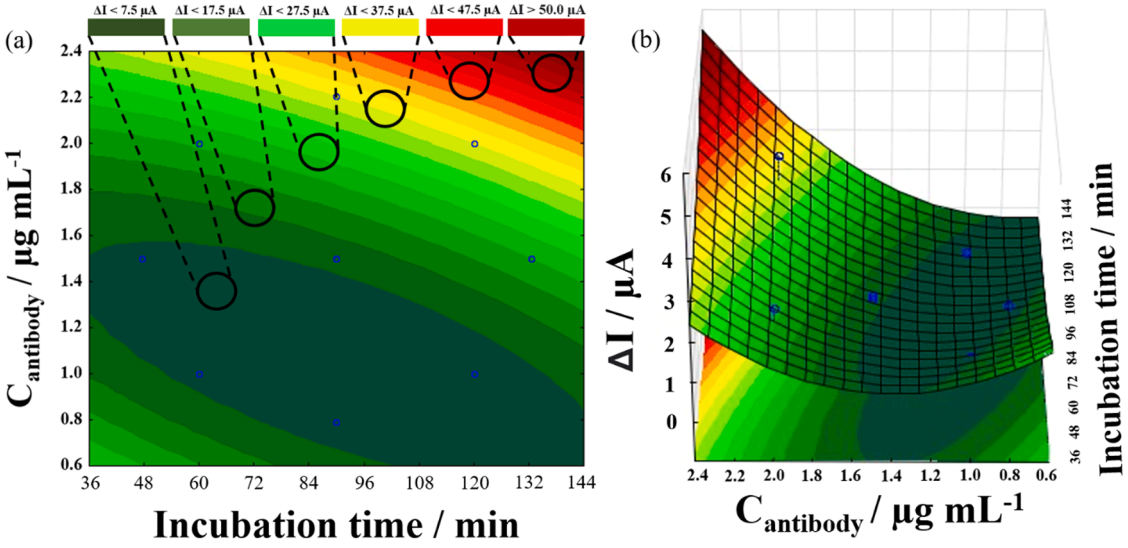

Fig. 5. (a) Level curve and (b) Surface response obtained for the optimization of the variables: antibody concentration (μg mL^{-1}) and incubation time (min) as a function of the current in the presence of antibody.

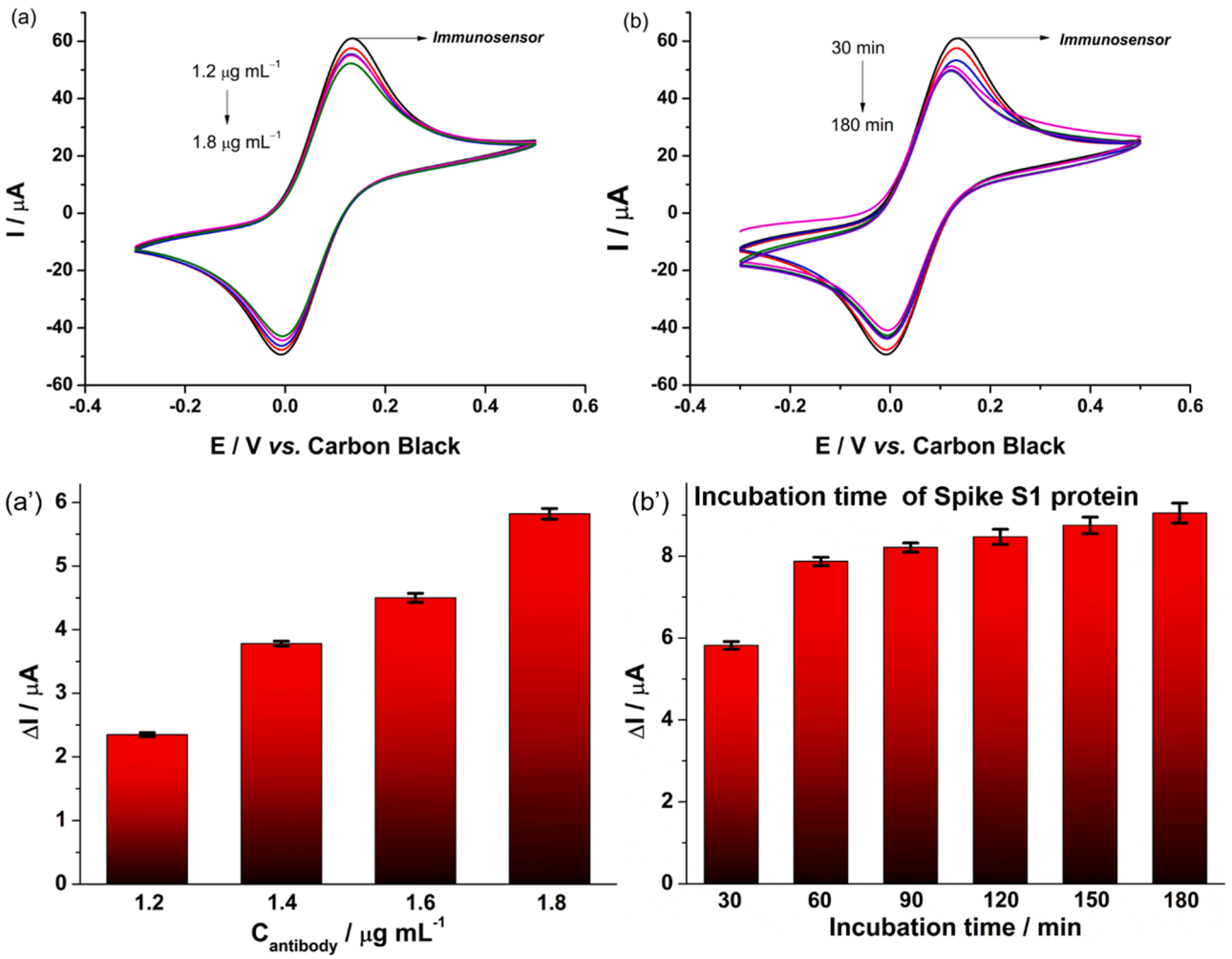

Fig. 6. Cyclic voltammograms recorded in the presence of 1.0 mmol L^{-1} FcMeOH in 0.1 mol L^{-1} KCl using the fabricated immunosensor for (a) antibody concentration (1.2; 1.4; 1.6 and 1.8 μg mL^{-1} and (b) incubation time (30; 60; 90; 120; 150 and 180 min); Scan rate: 50 mV s^{-1}). Bar column graph for optimizations of antibody concentration using a 30 min incubation time (a'), and incubation time of antigen using 1.8 μg mL^{-1} of antibody concentration (b').

After confirming the successful construction of the immunosensor, the optimization of the antibody immobilization step on the CB-PLA surface was performed. The evaluation of the other steps such as EDC: NHS binding and blocking with BSA was not performed since these are well-known and widely reported in the literature with fixed concentrations and times, these steps were not optimized [6,27,36]. The EDC: NHS was fixed in 10.0 mmol L^{-1} EDC and 20.0 mmol L^{-1} NHS in PBS 1x (pH = 7.4), and BSA solution in 1% w/v PBS 1x (pH = 7.4), with times of deposition of 1 h, and 30 min, respectively. The antibody immobilization was optimized for two variables, the concentration (μg mL^{-1}) and incubation time (min) of the antibody. For this, the multivariate optimization Central Composite Design was used. All peak current responses used for surface response construction were the difference between CB-PLA peak current in the presence and absence of antibodies. To monitor current differences (ΔI), 1.0 mmol L^{-1} FcMeOH in 0.1 mol L^{-1} KCl was used. Fig. 5 shows the response surface obtained in the optimization of the concentration of the antibody and incubation time.

Fig. 5 shows that as the concentration and incubation time of the antibody increases, there is a more accentuated current decay in the peaks, thus, a higher variation in current (ΔI) is observed. However, long incubation times are not favorable from the point of view of clinical tests, since the sensor production time will be longer, and increasing the antibody concentration indiscriminately increases the cost of production of the immunosensor. Furthermore, an expressive current decay possibly suggests that there is a greater partial "blockage" of the active sites. The excessive blocking of the active sites can hinder the analysis since it is necessary to have enough active sites to monitor the interactions between the receptor and antigen with the proposed redox probe. Another point to consider is that excess antibodies on the surface of the sensor, after binding with very low concentrations of protein, could saturate the surface and impair the performance of the immunosensor. Considering this, it is possible to observe that the time of 60 min of incubation provides a relatively satisfactory variation in the current response (ΔI). In addition, the study regarding antibody concentration was not satisfactory to indicate with precision the better value of concentration, however, it was possible to select a narrower range of antibody concentrations to assess the amount of antibody in the presence of the antigen.

Thus, using the selected incubation time, and to evaluate the response of the immunosensor in the presence of the antigen (spike S1 protein), a new optimization of antibody concentration was performed using univariate optimization after antigen incubation. For this study, an antigen concentration of 1.0 nmol L^{-1} was used, and the antibody concentration was evaluated at the concentrations of 1.2, 1.4, 1.6, and 1.8 μg mL^{-1}, using an incubation time of 60 min for antibody and 30 min for antigen. Employing the concentration value that provided an improved response, the time of incubation of the antigen was also evaluated (30, 60, 90, 120, 150, and 180 min). All optimization steps were monitored by cyclic voltammetry in the presence of 1.0 mmol L^{-1} FcMeOH in 0.1 mol L^{-1} KCl. Fig. 6 shows peak current responses for

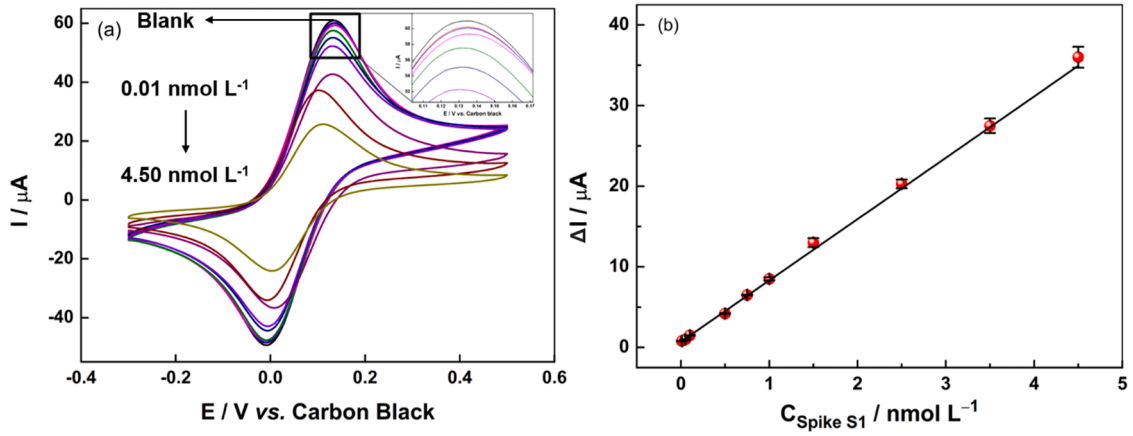

Fig. 7. Cyclic voltammograms recorded in presence of 1.0 mmol L^{-1} FcMeOH in 0.1 mol L^{-1} KCl using the fabricated immunosensor for increasing concentrations of antigen (0.01; 0.05; 0.1; 0.5; 0.75; 1.0; 1.5; 2.5; 3.5 and 4.5 nmol L^{-1}); Scan rate: 50 mV s^{-1}.

univariate optimization of antibody concentration in the presence of the antigen and antigen incubation time.

It can be seen in Fig. 6a that as the antibody concentration increases, there is an increase in the ΔI values. Thus, the concentration of 1.8 μg L^{-1} of antibody was chosen for further experiments. Regarding the incubation time (Fig. 6b), a similar behavior was noted, where the increase in the complexation time between the receptor (antibody) and the antigen (spike protein S1) provided higher variation in the peak current values. However, for more than 60 min of incubation, the increase in ΔI values is not significant, and the time of 60 min was chosen as the optimal time for the incubation of the antibody on the surface of the sensor.

The proposed immunosensor was applied in the detection of the spike S1 protein of the Coronavirus. For this, an analytical curve was constructed varying the antigen concentration (0.01; 0.05; 0.1; 0.5; 0.75; 1.0; 1.5; 2.5; 3.5 and 4.5 nmol L^{-1}). Each incubated concentration was monitored using cyclic voltammetry in the presence of 1.0 mmol L^{-1} FcMeOH in 0.1 mol L^{-1} KCl. Fig. 7 presents the voltammograms obtained for each concentration analyzed and the respective analytical curve obtained.

According to Fig. 7a, it is possible to observe that as the antigen concentration increases a proportionally higher current decay was observed, indicating that increased concentrations of antigen provided more blockage of the electrode surface, hindering the current transfer. Thus, it was possible to build an analytical curve with the concentrations 0.01; 0.05; 0.1; 0.5; 0.75; 1.0; 1.5; 2.5; 3.5 and 4.5 nmol L^{-1} (Fig. 7b). The construction of the analytical curve was carried out from the collection of anodic peak current values since it provided better linearity than cathodic peak current values ($R^2 = 0.817$), which was considered for further studies. The constructed curve showed a linear behavior, with an R^2 of 0.997 for anodic peak current values, demonstrating that the proposed immunosensor is capable of linearly responding to concentrations within the proposed working range. The equation of the curve obtained was ΔI (μA) = 0.707 + $C_{antigen}$ (nmol L^{-1}) × 7.606. The LOD and LOQ were calculated according to the following: LOD = $3.3\sigma_{intercept}/s$ and LOQ = 3 × LOD, where σ is the standard deviation of the intercept of the calibration curve, and "s" is the sensitivity (slope) of the calibration curve. The calculated LOD and LOQ values were 2.7 and 8.9 pmol L^{-1}, respectively.

Reproducibility tests of the construction of the immunosensor and stability of the analyses were also performed. For the reproducibility test, 5 different immunosensors were built and analyses were performed on each biosensor in the presence of 1.0 nmol L^{-1} antigen. For the immunosensor stability test, 10 consecutive scans were performed in the same biosensor, in the presence of 1.0 nmol L^{-1} antigen., which were carried out in the presence of 1.0 mmol L^{-1} FcMeOH in 0.1 mol L^{-1} KCl.

Table 1
Electrochemical immunosensors reported in the literature and their performance characteristics.

Sensor	Technique	Linear range (nmol L^{-1})	LOD (nmol L^{-1})	Ref.
3D Au/G-PLA	EIS[d]	50.0 – 500.0	6.8	[26]
3D-printed gold micropillars[a]	EIS	0.001 – 20.0	0.0000169	[41]
3D-printed Gpt-PLA	CV[e]	5.0 – 75.0	1.36	[27]
Pt/BioPET[b]	SWV[f]	0.0007 – 0.007	0.0007	[38]
Immunosensor	CV	30.0 – 150.0	2.53	[40]
Immunosensor	SWV	260.0 – 1040.0	260.0	[8]
Co-TNT sensor[c]	CA[g]	14.0 – 1400.0	0.7	[39]
3D-printed CB-PLA	CV	0.01 – 4.5	0.0027	This Work

[a] 3D-printed electrochemical immunosensor based on gold nanoparticles.
[b] platinum/biobased poly (ethylene terephthalate).
[c] cobalt-functionalized TiO2 nanotubes based electrochemical sensor.
[d] electrochemical impedance spectroscopy.
[e] Square Wave voltammetry.
[f] Cyclic voltammetry.
[g] chronoamperometry.

The reproducibility and stability tests showed a relative standard deviation (RSD) of 3.75 and 1.34%, respectively. Fig S2 shows the results obtained, in which the electrodes were kept at a low temperature (approximately 3 °C) and free of humidity. As can be seen in Figure S2a, from the tenth day onwards, the sensor's voltammetric profile changes, which may be related to the fact that they are 3D printed and are susceptible to change in behavior over time since these are produced from biodegradable and low-cost materials. However, according to Fig. S2, it can be seen that for up to 20 days, even with small changes in the response profiles, the current values remain statistically stable (RSD = 2.3%). Also, after 20 days the stability of the sensor declines (decay of 13.3% of the current peak, with an RSD of 12.3%.

The analytical characteristics obtained with the proposed 3D-printed immunosensor were compared with other immunosensors reported in the literature [8,26,27,37–40]. Table 1 presents some performance characteristics of the electrochemical immunosensors described in the literature.

The literature shows several electrochemical immunosensors applied to the detection of the SARS-CoV-2 virus, and Table 1 highlights some examples. It is possible to infer that the immunosensor presented in this work reached good analytical characteristics, comparable to the observed in the literature. In addition, the possibility of excluding stages in the production of the proposed immunosensor makes it simpler, facilitating preparation and not requiring specialized operators for

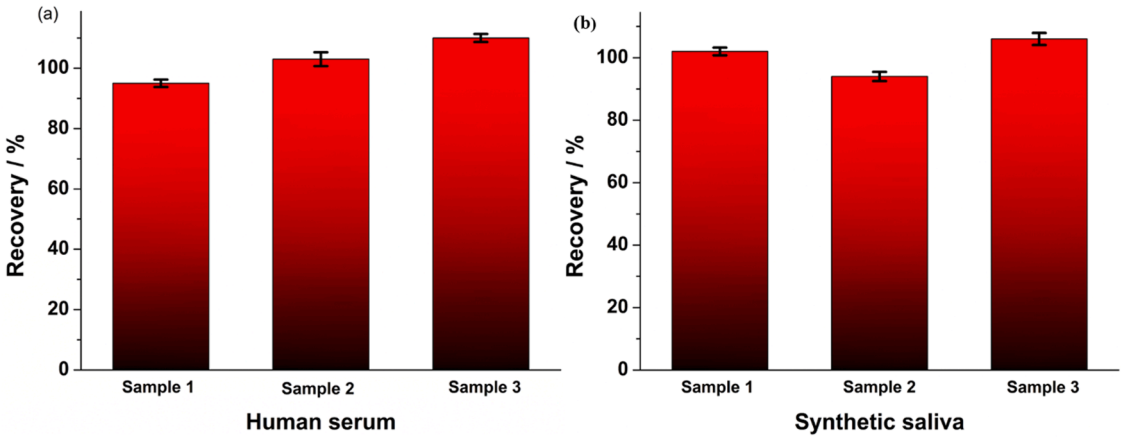

Fig. 8. Bar graph of recoveries response in the percentage of the antigen in human serum (a) and synthetic saliva (b) samples. Concentrations: samples 1, 2, and 3 = 0.05; 0.1 and 1.0 nmol L^{-1}, respectively.

production. It is important to note that for the development of the present immunosensor, it was not necessary to modify the surface with metallic particles or similar materials.

The immunosensor was optimized by using the multivariate method and univariate procedures. The response of the immunosensor presented in this work can be considered excellent, as eliminating modification steps and maintaining good analytical characteristics is fundamental for the creation of more robust clinical tests with high potential for use. In this context, multivariate optimization proved to be highly effective, indicating ideal operating parameters and allowing the immunosensor to perform to its full potential. Another crucial point to highlight is that the proposed immunosensor has carbon black as the conductive material base, which is inexpensive compared to others such as graphene, graphite, and platinum, commonly reported for the manufacture of immunosensors. Indeed, the electrochemical proposed immunosensor is a viable alternative for clinical analysis centers, since it is built easily, directly, and in an automatized way from 3D printing technology, and the platform proposed requires only a small sample volume to perform the analyses (100 μL).

To demonstrate the efficiency of the 3D-printed immunosensor, the analysis of real and synthetic samples was performed. For this, human serum and synthetic saliva samples were fortified with three known concentrations (0.05, 0.1, and 1.0 nmol L^{-1}) of the antigen, and subsequently incubated on the electrode surface. Fig. 8. presents the recoveries values obtained for all analyzed samples.

The recovery values obtained ranged from 92.0 to 105.0%, inferring that all the analyses carried out did not show a significant matrix effect. In addition, according to the tests carried out on the samples, the sensor can be presented as a viable and practical alternative for clinical testing. The use of 3D-printing technology to provide the complete platform is a differential for it allows the design exactly as idealized and desired. Thus, attributing important characteristics for point-of-care devices, such as miniaturization, which allow the use of low amounts of samples, the portability to the system, and adaptability of materials, either attributing low-cost, flexibility/rigidness, or even improved materials. Regarding the materials, the possibility to obtain conductive filaments for 3D printing in a laboratory can be differential given the need for the importation of conductive filaments, which in some cases is difficulted, is eliminated. In addition, different materials can be employed to attribute varied characteristics to the final sensor. In this case, carbon black was used to attribute low cost, making the proposed platform very accessible, given the high importance of testing for the SARS-CoV-2 virus.

Conclusion

Through 3D printing and the use of a lab-made conductive filament based on carbon black and PLA, it was possible to build successfully an electrochemical immunosensor, based on covalent linking of EDC:NHS directly at the electrode surface, for the detection of Spike S1 protein in human serum synthetic saliva samples. The immunosensor showed satisfactory results with a low LOD of 2.7 pmol L^{-1} and high sensitivity (7.606 μA $nmol^{-1}$ L). Adequate recovery values in the proposed samples ranged from 92.0 to 105.0%, demonstrating good applicability and no significant matrix effect. Given this, the 3D printed immunosensor developed in the present work links the qualities of 3D printing with those of electrochemical sensors. Furthermore, the sensor produced is portable and applied entirely with portable equipment. In this way, the present immunosensor can be employed as an alternative to the existing tests, being able to be applied in loco, in a simple yet fast way.

Declaration of Competing Interest

The authors declare that they have no known competing financial interests or personal relationships that could have appeared to influence the work reported in this paper.

Data availability

No data was used for the research described in the article.

Acknowledgments

The authors are grateful to the Brazilian agencies CAPES (001 and 88887.504861/2020-00) FAPESP (2017/21097-3; and 2022/06145-0), CNPq (301796/2022-0; 380632/2023-3) for the financial support.

Supplementary materials

Supplementary material associated with this article can be found, in the online version, at doi:10.1016/j.talo.2023.100250.

References

[1] A. Kumar, P.K. Gupta, A. Srivastava, A review of modern technologies for tackling COVID-19 pandemic, Diabetes Metab. Syndr. Clin. Res. Rev. 14 (2020) 569–573, https://doi.org/10.1016/J.DSX.2020.05.008.

[2] V. Ong, A. Soleimani, F. Amirghasemi, S.K. Nejad, M. Abdelmonem, M. Razaviyayn, P. Hosseinzadeh, L. Comai, M.P.S. Mousavi, Impedimetric sensing: an emerging tool for combating the COVID-19 pandemic, Biosens 13 (2023) 204, https://doi.org/10.3390/BIOS13020204. Page13 (2023) 204.

[3] B. Long, B.M. Carius, S. Chavez, S.Y. Liang, W.J. Brady, A. Koyfman, M. Gottlieb, Clinical update on COVID-19 for the emergency clinician: presentation and evaluation, Am. J. Emerg. Med. 54 (2022) 46–57, https://doi.org/10.1016/J.AJEM.2022.01.028.
[4] M. Pradhan, K. Shah, A. Alexander, Ajazuddin, S.Minz, M.R. Singh, D. Singh, K. Yadav, N.S. Chauhan, COVID-19: clinical presentation and detection methods, 43 (2021). doi:10.1080/15321819.2021.1951291.
[5] O. Filchakova, D. Dossym, A. Ilyas, T. Kuanysheva, A. Abdizhamil, R. Bukasov, Review of COVID-19 testing and diagnostic methods, Talanta 244 (2022), 123409, https://doi.org/10.1016/J.TALANTA.2022.123409.
[6] L.C. Brazaca, P.L. dos Santos, P.R. de Oliveira, D.P. Rocha, J.S. Stefano, C. Kalinke, R.A. Abarza Muñoz, J.A. Bonacin, B.C. Janegitz, E. Carrilho, Biosensing strategies for the electrochemical detection of viruses and viral diseases – a review, Anal. Chim. Acta. 1159 (2021), 338384, https://doi.org/10.1016/J.ACA.2021.338384.
[7] S. Madhurantakam, S. Muthukumar, S. Prasad, Emerging electrochemical biosensing trends for rapid diagnosis of COVID-19 biomarkers as point-of-care platforms: a critical review, ACS Omega 7 (2022) 12467–12473, https://doi.org/10.1021/ACSOMEGA.2C00638/ASSET/IMAGES/LARGE/AO2C00638_0003.JPEG.
[8] B. Mojsoska, S. Larsen, D.A. Olsen, J.S. Madsen, I. Brandslund, F.A. Alatraktchi, Rapid SARS-CoV-2 detection using electrochemical immunosensor, Sensors 21 (2021) 390, https://doi.org/10.3390/s21020390.
[9] N. Kumar, N.P. Shetti, S. Jagannath, T.M. Aminabhavi, Electrochemical sensors for the detection of SARS-CoV-2 virus, Chem. Eng. J. 430 (2022), 132966, https://doi.org/10.1016/J.CEJ.2021.132966.
[10] Z. Zhang, P. Ma, R. Ahmed, J. Wang, D. Akin, F. Soto, B.F. Liu, P. Li, U. Demirci, Advanced point-of-care testing technologies for human acute respiratory virus detection, Adv. Mater. 34 (2022), 2103646, https://doi.org/10.1002/ADMA.202103646.
[11] L.R.G. Silva, A. Gevaerd, L.H. Marcolino-Junior, M.F. Bergamini, T.A. Silva, B. C. Janegitz, 3D-printed electrochemical devices for sensing and biosensing of biomarkers, Adv. Bioelectrochem. 2 (2022) 121–136, https://doi.org/10.1007/978-3-030-95270-9_7.
[12] A. Gevaerd, L.R.G. Silva, T.A. Silva, L.H. Marcolino-Junior, M.F. Bergamini, B. C. Janegitz, Screen-printed electrochemical sensors and biosensors for detection of biomarkers, Adv. Bioelectrochem. 3 (2022) 113–140, https://doi.org/10.1007/978-3-030-97921-8_5.
[13] G.C. Biswas, S. Choudhury, M.M. Rabbani, J. Das, A review on potential electrochemical point-of-care tests targeting pandemic infectious disease detection: COVID-19 as a reference, Chemosens 10 (2022) 269, https://doi.org/10.3390/CHEMOSENSORS10070269. Page10 (2022) 269.
[14] J.S. Stefano, L.O. Orzari, H.A. Silva-Neto, V.N. de Ataíde, L.F. Mendes, W.K. T. Coltro, T.R. Longo Cesar Paixão, B.C. Janegitz, Different approaches for fabrication of low-cost electrochemical sensors, Curr. Opin. Electrochem. 32 (2022), 100893, https://doi.org/10.1016/j.coelec.2021.100893.
[15] Y. Zhang, N. Zhou, Electrochemical biosensors based on micro-fabricated devices for point-of-care testing: a review, Electroanalysis 34 (2022) 168–183, https://doi.org/10.1002/ELAN.202100281.
[16] J.S. Stefano, C. Kalinke, R.G. da Rocha, D.P. Rocha, V.A.O.P. da Silva, J.A. Bonacin, L. Angnes, E.M. Richter, B.C. Janegitz, R.A.A. Muñoz, Electrochemical (bio)sensors enabled by fused deposition modeling-based 3D printing: a guide to selecting designs, printing parameters, and post-treatment protocols, Anal. Chem. (2022), https://doi.org/10.1021/ACS.ANALCHEM.1C05523 acs.analchem.1c05523.
[17] M.J. Whittingham, R.D. Crapnell, E.J. Rothwell, N.J. Hurst, C.E. Banks, Additive manufacturing for electrochemical labs: an overview and tutorial note on the production of cells, electrodes and accessories, Talanta Open 4 (2021), 100051, https://doi.org/10.1016/J.TALO.2021.100051.
[18] R.M. Cardoso, C. Kalinke, R.G. Rocha, P.L. dos Santos, D.P. Rocha, P.R. Oliveira, B. C. Janegitz, J.A. Bonacin, E.M. Richter, R.A.A. Munoz, Additive-manufactured (3D-printed) electrochemical sensors: a critical review, Anal. Chim. Acta. 1118 (2020) 73–91, https://doi.org/10.1016/J.ACA.2020.03.028.
[19] J.S. Stefano, L.R.G.E. Silva, B.C. Janegitz, New carbon black-based conductive filaments for the additive manufacture of improved electrochemical sensors by fused deposition modeling, Mikrochim. Acta. 189 (2022) 414, https://doi.org/10.1007/S00604-022-05511-2.
[20] R.G. Rocha, R.M. Cardoso, P.J. Zambiazi, S.V.F. Castro, T.V.B. Ferraz, G. de O. Aparecido, J.A. Bonacin, R.A.A. Munoz, E.M. Richter, Production of 3D-printed disposable electrochemical sensors for glucose detection using a conductive filament modified with nickel microparticles, Anal. Chim. Acta. 1132 (2020) 1–9, https://doi.org/10.1016/j.aca.2020.07.028.
[21] L.R. Guterres Silva, J. Santos Stefano, R. Cornélio Ferreira Nocelli, B. Campos Janegitz, 3D electrochemical device obtained by additive manufacturing for sequential determination of paraquat and carbendazim in food samples, Food Chem 406 (2023), 135038, https://doi.org/10.1016/J.FOODCHEM.2022.135038.
[22] V.A.O.P. Silva, W.S. Fernandes-Junior, D.P. Rocha, J.S. Stefano, R.A.A. Munoz, J. A. Bonacin, B.C. Janegitz, 3D-printed reduced graphene oxide/polylactic acid electrodes: a new prototyped platform for sensing and biosensing applications, Biosens. Bioelectron. 170 (2020), 112684, https://doi.org/10.1016/J.BIOS.2020.112684.
[23] R.M. Cardoso, C. Kalinke, R.G. Rocha, P.L. dos Santos, D.P. Rocha, P.R. Oliveira, B. C. Janegitz, J.A. Bonacin, E.M. Richter, R.A.A. Munoz, Additive-manufactured (3D-printed) electrochemical sensors: a critical review, Anal. Chim. Acta. 1118 (2020) 73–91, https://doi.org/10.1016/j.aca.2020.03.028.
[24] A. Ambrosi, M. Pumera, 3D-printing technologies for electrochemical applications, Chem. Soc. Rev. 45 (2016) 2740–2755, https://doi.org/10.1039/C5CS00714C.
[25] G. Martins, J.L. Gogola, L.H. Budni, B.C. Janegitz, L.H. Marcolino-Junior, M. F. Bergamini, 3D-printed electrode as a new platform for electrochemical immunosensors for virus detection, Anal. Chim. Acta. 1147 (2021) 30–37, https://doi.org/10.1016/j.aca.2020.12.014.
[26] J. Muñoz, M. Pumera, 3D-Printed COVID-19 immunosensors with electronic readout, Chem. Eng. J. 425 (2021), 131433, https://doi.org/10.1016/J.CEJ.2021.131433.
[27] J.S. Stefano, L.R. Guterres e Silva, R.G. Rocha, L.C. Brazaca, E.M. Richter, R. A. Abarza Muñoz, B.C. Janegitz, New conductive filament ready-to-use for 3D-printing electrochemical (bio)sensors: towards the detection of SARS-CoV-2, Anal. Chim. Acta. (2021), 339372, https://doi.org/10.1016/J.ACA.2021.339372.
[28] C. Kalinke, R.D. Crapnell, E. Sigley, M.J. Whittingham, P.R. de Oliveira, L. C. Brazaca, B.C. Janegitz, J.A. Bonacin, C.E. Banks, Recycled additive manufacturing feedstocks with carboxylated multi-walled carbon nanotubes toward the detection of yellow fever virus cDNA, Chem. Eng. J. 467 (2023), 143513, https://doi.org/10.1016/J.CEJ.2023.143513.
[29] F. de Matos Morawski, G. Martins, M.K. Ramos, A.J.G. Zarbin, L. Blanes, M. F. Bergamini, L.H. Marcolino-Junior, A versatile 3D printed multi-electrode cell for determination of three COVID-19 biomarkers, Anal. Chim. Acta. 1258 (2023), 341169, https://doi.org/10.1016/J.ACA.2023.341169.
[30] D.E. Romonti, A.V. Gomez Sanchez, I. Milošev, I. Demetrescu, S. Ceré, Effect of anodization on the surface characteristics and electrochemical behaviour of zirconium in artificial saliva, Mater. Sci. Eng. C. 62 (2016) 458–466, https://doi.org/10.1016/J.MSEC.2016.01.079.
[31] R.D. Crapnell, A. Garcia-Miranda Ferrari, M.J. Whittingham, E. Sigley, N.J. Hurst, E.M. Keefe, C.E. Banks, Adjusting the connection length of additively manufactured electrodes changes the electrochemical and electroanalytical performance, Sensors 22 (2022) 9521, https://doi.org/10.3390/S22239521. Page22 (2022) 9521.
[32] D.P. Rocha, V.N. Ataide, A. de Siervo, J.M. Gonçalves, R.A.A. Muñoz, T.R.L. C. Paixão, L. Angnes, Reagentless and sub-minute laser-scribing treatment to produce enhanced disposable electrochemical sensors via additive manufacture, Chem. Eng. J. 425 (2021), 130594, https://doi.org/10.1016/j.cej.2021.130594.
[33] A.G.M. Ferrari, C.W. Foster, P.J. Kelly, D.A.C. Brownson, C.E. Banks, Determination of the electrochemical area of screen-printed electrochemical sensing platforms, Biosens 8 (2018) 53, https://doi.org/10.3390/BIOS8020053. Page8 (2018) 53.
[34] C. Amatore, N.Da Mota, C. Sella, L. Thouin, Theory and experiments of transport at channel microband electrodes under laminar flows. 1. Steady-state regimes at a single electrode, Anal. Chem. 79 (2007) 8502–8510, https://doi.org/10.1021/AC070971Y.
[35] T. Beduk, D. Beduk, J.I. de Oliveira Filho, F. Zihnioglu, C. Cicek, R. Sertoz, B. Arda, T. Goksel, K. Turhan, K.N. Salama, S. Timur, Rapid point-of-care COVID-19 diagnosis with a gold-nanoarchitecture-assisted laser-scribed graphene biosensor, Anal. Chem. 93 (2021) 8585–8594, https://doi.org/10.1021/ACS.ANALCHEM.1C01444/ASSET/IMAGES/LARGE/AC1C01444_0006.JPEG.
[36] G.C.M. de Oliveira, J.H. de S. Carvalho, L.C. Brazaca, N.C.S. Vieira, B.C. Janegitz, Flexible platinum electrodes as electrochemical sensor and immunosensor for Parkinson's disease biomarkers, Biosens. Bioelectron. 152 (2020), 112016, https://doi.org/10.1016/j.bios.2020.112016.
[37] M.A. Ali, C. Hu, S. Jahan, B. Yuan, M.S. Saleh, E. Ju, S.J. Gao, R. Panat, Sensing of COVID-19 antibodies in seconds via aerosol jet nanoprinted reduced-graphene-oxide-coated 3D electrodes, Adv. Mater. (2020), 2006647, https://doi.org/10.1002/adma.202006647.
[38] R.V. Blasques, P.R. de Oliveira, C. Kalinke, L.C. Brazaca, R.D. Crapnell, J. A. Bonacin, C.E. Banks, B.C. Janegitz, Flexible label-free platinum and Bio-PET-based immunosensor for the detection of SARS-CoV-2, Biosens 13 (2023) 190, https://doi.org/10.3390/BIOS13020190. Page13 (2023) 190.
[39] B.S. Vadlamani, T. Uppal, S.C. Verma, M. Misra, Functionalized TiO2 nanotube-based electrochemical biosensor for rapid detection of SARS-CoV-2, Sensors 20 (2020) 5871, https://doi.org/10.3390/S20205871. Page20 (2020) 5871.
[40] V. Liustrovaite, M. Drobysh, A. Rucinskiene, A. Baradoke, A. Ramanaviciene, I. Plikusiene, U. Samukaite-Bubniene, R. Viter, C.-F. Chen, A. Ramanavicius, Towards an electrochemical immunosensor for the detection of antibodies against SARS-CoV-2 spike protein, J. Electrochem. Soc. 169 (2022), 037523, https://doi.org/10.1149/1945-7111/AC5D91.
[41] M. Azahar Ali, C. Hu, S. Jahan, B. Yuan, M. Sadeq Saleh, E. Ju, S.-J. Gao, R. Panat, M.A. Ali, C. Hu, S. Jahan, B. Yuan, M.S. Saleh, R. Panat, E. Ju, S. Gao, Cancer Virology program, sensing of COVID-19 antibodies in seconds via aerosol jet nanoprinted reduced-graphene-oxide-coated 3D electrodes, Adv. Mater. 33 (2021), 2006647, https://doi.org/10.1002/ADMA.202006647.

Luiz Ricardo Guterres Silva: PhD student in Materials Sciences at the Federal University of São Carlos under the guidance of Prof. Dr. Bruno Campos Janegitz. He has a master's degree in Chemistry (Electrochemistry and Electroanalytical) and a degree in Chemistry from the Federal University of Espírito Santo. He has experience in the area of Materials Science and Chemistry, with emphasis on Electroanalytical/Electrochemistry, working mainly on the following topics: development of conductive composites for 3D printing, 3D printed (bio)sensors, screen printed electrodes and new 3D printed architectures for electroanalytical.

Jéssica Santos Stefano is graduated in Chemistry from the Federal University of Uberlândia in 2014, and achieved her master (2016) and Ph.D. degree (2020) at the same University in the Analytical Chemistry area with an internship period at the Ruhr-Universität Bochum, DE (2018–2019). She is currently a postdoctoral researcher at Federal University of São Carlos. She has experience on modified electrodes with carbon nanomaterials, such as carbon nanotubes, and their application in hydrodynamic systems, such as batch-injection and flow-injection analysis, as well as with bipolar electrochemistry, fabrication of conductive filaments and obtention and application of 3D printed electrochemical (bio)sensors.

Robert Crapnell is Senior Research Associate at Manchester Metropolitan University in Professor Craig E. Banks research group. His-has Research focusing around Additive Manufacturing, Electrochemistry, Circular Economy, Electroanalysis, Electrolysis and Energy Storage.

Craig E. Banks holds a personal chair in nano- and electrochemical technology and has published over 500 papers and works on next generation screen printed electrochemical sensing platforms as well the use of additive manufacturing in water splitting, sensor design, supercapacitors, and battery development.

Bruno Campos Janegitz received Ph.D. degree from Federal University of São Carlos, in 2012. He was a postdoctoral researcher at University of São Paulo between 2012 and 2014. At present, he is Professor at Federal University of São Carlos. His-research interests include electroanalytical chemistry, nanostructured electrode materials and modified electrode surfaces, electrochemical sensors and biosensors for medical and environmental analysis.